Vol 18 No 8, August 2009
1674-1056/2009/18(08)/3183-06

Chinese Physics B

© 2009 Chin. Phys. Soc.
and IOP Publishing Ltd

Mode field diameter and nonlinear properties of air-core nanowires*

Hu Xiao-Hong(胡晓鸿)[a)b)], Zhao Wei(赵 卫)[a)], Gong Yong-Kang(宫永康)[a)], Wang Lei-Ran(王擂然)[a)], Lu Ke-Qing(卢克清)[a)], and Liu Xue-Ming(刘雪明)[a)†]

[a)] *State Key Laboratory of Transient Optics and Photonics, Xi'an Institute of Optics and Precision Mechanics, Chinese Academy of Sciences, Xi'an* 710119, *China*

[b)] *Graduate School of the Chinese Academy of Sciences, Beijing* 100049, *China*

(Received 30 June 2008; revised manuscript received 29 October 2008)

Exact solutions of Maxwell's equations describing the lightwave through 3-layer-structured cylindrical waveguide are obtained and the mode field diameter and nonlinear coefficient of air-core nanowires (ACNWs) are numerically calculated. The simulation results show that ACNWs offer some unique optical properties, such as tight field confining ability and extremely high nonlinearity. At a certain wavelength and air core radius, we optimize the waveguide design to maximize the nonlinear coefficient and minimize the mode field diameter. Our results show that the ACNWs may be powerful potential tools for novel micro-photonic devices in the near future.

Keywords: waveguides, nanowires, numerical calculation, fiber optics
PACC: 0350D, 4110H, 4281, 4281D

1. Introduction

Conventional optical fibers, whose diameter ranges from micrometer to millimeter, have been adequately researched and successfully applied to many fields such as optical communication, optical sensing and optical power delivery systems.[1,2] Recently, dielectric sub-micrometer- and nanometer-diameter wires have attracted more and more attention and their basic optical properties, such as field distribution, power distribution and dispersion character, have been studied widely.[3−8] Meanwhile some types of low-loss wires have been fabricated successfully.[9,10] These wires are about tens to thousands of times thinner than the commonly used micrometer-diameter waveguides. They will be promising components in future micro-photonic devices for various applications, such as optical communications and optical sensing.[9] Particularly according to Refs.[11] and [12], air-core nanowire (ACNW) will be available in the near future and it will provide many opportunities for the realization of miniaturized high performance and novel photonic devices.

In this paper, exact solutions of Maxwell's equations describing the lightwave propagation through ACNWs are achieved and the mode field diameter (MFD) and nonlinear coefficients of the ACNWs are numerically simulated MFD gives the effective spot diameter of fundamental mode and is the measurement of the field confinement ability of optical fiber. For many nonlinear optical processes, e.g., supercontinuum generation, it is desirable to maximize the nonlinear coefficient. In our study, we have optimized the ACNW design to achieve the maximum nonlinearity and tight light confinement. The simulation results show that ACNWs could facilitate the development of optical waveguides for ultra-low-threshold nonlinear processes.

2. Theoretical model

We assume that the wire is ideally uniform in diameter and smooth in sidewall. The refractive index profile of ACNW is schematically illustrated in Fig.1.[3] There are three regions in the cross section: a hollow core with radius a, a dielectric region with radius b, and the infinite air cladding. The refractive indices of the core, dielectric region and the outermost cladding are defined as n_1, n_2 and n_3 respectively.

*Project supported by the "Hundreds of Talents Programs" of the Chinese Academy of Sciences and by the National Natural Science Foundation of China (Grant Nos 10874239, 10604066 and 60537060).
†Corresponding author. E-mail: liuxm@opt.ac.cn, liuxueming72@yahoo.com

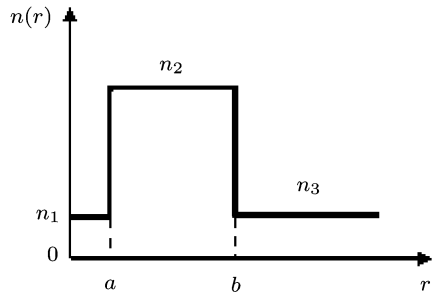


Fig.1. Refractive index profile of the ACNW.

After solving the Helmholtz equations, longitudinal field components can be given by:[3]

$$E_z = \begin{cases} A\,\mathrm{I}_m(u_1 r) f_c, & 0 < r < a \\ [B\,\mathrm{J}_m(u_2 r) + C\mathrm{Y}_m(u_2 r)]\, f_c, & a < r < b \\ D\,\mathrm{K}_m(u_3 r) f_c, & r > b \end{cases}, \tag{1}$$

$$H_z = \begin{cases} A'\mathrm{I}_m(u_1 r) f_s, & 0 < r < a \\ [B'\mathrm{J}_m(u_2 r) + C'\mathrm{Y}_m(u_2 r)]\, f_s, & a < r < b \\ D'\mathrm{K}_m(u_3 r) f_s, & r > b \end{cases}, \tag{2}$$

where J_m and Y_m are the first-kind and second-kind Bessel functions respectively, and I_m and K_m are the corresponding first-kind and second-kind modified-Bessel functions respectively. $u_1 = (\beta^2 - k_0^2 n_1^2)^{1/2}$, $u_2 = (k_0^2 n_2^2 - \beta^2)^{1/2}$, $u_3 = (\beta^2 - k_0^2 n_3^2)^{1/2}$, $f_c = \cos(m\phi + \varphi_m)\exp[j(wt - \beta z)]$, and $f_s = \sin(m\phi + \varphi_m)\exp[j(wt - \beta z)]$. β is the propagation constant and $k_0 = 2\pi/\lambda$ is the free space wave number.

Substitute the expressions of E_z and H_z into the following equations:[3]

$$E_r = -\frac{j}{k_0^2 n^2 - \beta^2}\left(\beta\frac{\partial E_z}{\partial r} + \frac{w\mu_0}{r}\frac{\partial H_z}{\partial \phi}\right), \tag{3a}$$

$$E_\phi = -\frac{j}{k_0^2 n^2 - \beta^2}\left(\frac{\beta}{r}\frac{\partial E_z}{\partial \phi} - w\mu_0\frac{\partial H_z}{\partial r}\right), \tag{3b}$$

$$H_r = -\frac{j}{k_0^2 n^2 - \beta^2}\left(\beta\frac{\partial H_z}{\partial r} - \frac{w\varepsilon_0 n^2}{r}\frac{\partial E_z}{\partial \phi}\right), \tag{3c}$$

$$H_\phi = -\frac{j}{k_0^2 n^2 - \beta^2}\left(\frac{\beta}{r}\frac{\partial H_z}{\partial \phi} + w\varepsilon_0 n^2\frac{\partial E_z}{\partial r}\right). \tag{3d}$$

The transverse components of the field can be expressed as follows:

$$E_r = \begin{cases} \dfrac{j}{u_1^2}\left[A\beta u_1 \mathrm{I}'_m(u_1 r) + A'\dfrac{w\mu_0}{r} m\,\mathrm{I}_m(u_1 r)\right], & 0 < r < a, \\ -\dfrac{j}{u_2^2}\left[B\beta u_2 \mathrm{J}'_m(u_2 r) + C\beta u_2 \mathrm{Y}'_m(u_2 r) + B'\dfrac{mw\mu_0}{r}\mathrm{J}_m(u_2 r) + C'\dfrac{mw\mu_0}{r}\mathrm{Y}_m(u_2 r)\right], & a < r < b, \\ \dfrac{j}{u_3^2}\left[D\beta u_3 \mathrm{K}'_m(u_3 r) + D'\dfrac{mw\mu_0}{r}\mathrm{K}_m(u_3 r)\right], & r > b \end{cases} \tag{4a}$$

$$H_\phi = \begin{cases} -\dfrac{j}{u_1^2}\left[A\dfrac{m\beta}{r}\mathrm{I}_m(u_1 r) + A' w\mu_0 u_1 \mathrm{I}'_m(u_1 r)\right], & 0 < r < a, \\ \dfrac{j}{u_2^2}\left[B\dfrac{m\beta}{r}\mathrm{J}_m(u_2 r) + C\dfrac{m\beta}{r}\mathrm{Y}_m(u_2 r) + B' w\mu_0 u_2 \mathrm{J}'_m(u_2 r) + C' w\mu_0 u_2 \mathrm{Y}'_m(u_2 r)\right], & a < r < b, \\ -\dfrac{j}{u_3^2}\left[D\dfrac{m\beta}{r}\mathrm{K}_m(u_3 r) + D' w\mu_0 u_3 \mathrm{K}'_m(u_3 r)\right], & r > b \end{cases} \tag{4b}$$

$$H_r = \begin{cases} \dfrac{j}{u_1^2}\left[A\dfrac{mw\varepsilon_0 n_1^2}{r} I_m(u_1 r) + A'\beta u_1 \mathrm{I}'_m(u_1 r)\right], & 0 < r < a, \\ -\dfrac{j}{u_2^2}\left[B\dfrac{mw\varepsilon_0 n_2^2}{r}\mathrm{J}_m(u_2 r) + C\dfrac{mw\varepsilon_0 n_2^2}{r}\mathrm{Y}_m(u_2 r) + B'\beta u_2 \mathrm{J}'_m(u_2 r) + C'\beta u_2 \mathrm{Y}'_m(u_2 r)\right], & a < r < b, \\ \dfrac{j}{u_3^2}\left[D\dfrac{mw\varepsilon_0 n_3^2}{r}\mathrm{K}_m(u_3 r) + D'\beta u_3 \mathrm{K}'_m(u_3 r)\right], & r > b \end{cases} \tag{4c}$$

$$H_\phi = \begin{cases} \dfrac{j}{u_1^2}\left[Aw\varepsilon_0 n_1^2 u_1 \mathrm{I}'_m(u_1 r) + A'\dfrac{m\beta}{r}\mathrm{I}_m(u_1 r)\right], & 0 < r < a, \\ -\dfrac{j}{u_2^2}\left[Bw\varepsilon_0 n_2^2 u_2 \mathrm{J}'_m(u_2 r) + Cw\varepsilon_0 n_2^2 u_2 \mathrm{Y}'_m(u_2 r) + B'\dfrac{m\beta}{r}\mathrm{J}_m(u_2 r) + C'\dfrac{m\beta}{r}\mathrm{Y}_m(u_2 r)\right], & a < r < b, \\ \dfrac{j}{u_3^2}\left[Dw\varepsilon_0 n_3^2 u_3 \mathrm{K}'_m(u_3 r) + D'\dfrac{m\beta}{r}\mathrm{K}_m(u_3 r)\right]. & r > b. \end{cases} \tag{4d}$$

For simplicity, the common factors $f_c = \cos(m\phi + \varphi_m)\exp[j(wt - \beta z)]$ related to E_r and H_ϕ, and $f_s = \sin(m\phi + \varphi_m)\exp[j(wt - \beta z)]$ related to E_ϕ and H_r have been omitted.

Using the boundary conditions that the tangential components of the electromagnetic field (E_ϕ, E_z, H_ϕ, H_z) must be continuous at the inner and outer cylinder surfaces ($r = a$ and $r = b$), a system of eight linear homogeneous equations is obtained. These equations satisfy the eight coefficients of the electromagnetic field components. In order to obtain a set of non-zero solutions for the eight coefficients, the determinant of the homogeneous equations must be equal to zero:

$$\det[M(\beta)] = 0, \tag{5}$$

where M is the resulting matrix of the system of linear homogeneous equations. Here we consider the situation of fundamental mode and thus set $m = 1$ in Eqs.(1)–(4).

With the propagation constant obtained by numerically solving Eq.(5), we can then numerically solve the homogeneous equations and obtain the eight coefficients (A, B, C, D, A', B', C', D'). As a result, all the field components can be calculated.

Using electromagnetic field components (E_r, E_ϕ, H_r, H_ϕ), the z components of Poynting vectors are obtained

$$\begin{aligned} S_z &= \frac{1}{2}\Re(E_r H_\phi^* - E_\phi H_r^*) \\ &= \frac{1}{2}\Re(E_r H_\phi^* \cos^2\phi - E_\phi H_r^* \sin^2\phi) \\ &= \frac{1}{4}\Re[(E_r H_\phi^* - E_\phi H_r^*) \\ &\quad + (E_r H_\phi^* + E_\phi H_r^*)\cos 2\phi]. \end{aligned} \tag{6}$$

Here, we have set the initial phase $\varphi_1 = 0$.

Finally, the MFD and effective nonlinear coefficient γ are obtained[5]

$$\begin{aligned} \mathrm{MFD} &= 2\sqrt{2}\sqrt{\frac{\int S_z r^2 \mathrm{d}^2 r}{\int S_z \mathrm{d}^2 r}} \\ &= 2\sqrt{2}\sqrt{\frac{\int_0^a S_{z1} r^2 r\mathrm{d}r \int_0^{2\pi}\mathrm{d}\phi + \int_a^b S_{z2} r^2 r\mathrm{d}r \int_0^{2\pi}\mathrm{d}\phi + \int_b^\infty S_{z3} r^2 r\mathrm{d}r \int_0^{2\pi}\mathrm{d}\phi}{\int_0^a S_{z1} r\mathrm{d}r \int_0^{2\pi}\mathrm{d}\phi + \int_a^b S_{z2} r\mathrm{d}r \int_0^{2\pi}\mathrm{d}\phi + \int_b^\infty S_{z3} r\mathrm{d}r \int_0^{2\pi}\mathrm{d}\phi}}, \end{aligned} \tag{7}$$

$$\begin{aligned} \gamma &= \frac{2\pi}{\lambda}\cdot\frac{\int n_2 S_z^2 \mathrm{d}^2 r}{(\int S_z \mathrm{d}^2 r)^2} \\ &\approx \frac{2\pi}{\lambda}\cdot\frac{\int_a^b n_2 S_{z2}^2 r\mathrm{d}r \int_0^{2\pi}\mathrm{d}\phi}{\left(\int_0^a S_{z1} r\mathrm{d}r \int_0^{2\pi}\mathrm{d}\phi + \int_a^b S_{z2} r\mathrm{d}r \int_0^{2\pi}\mathrm{d}\phi + \int_b^\infty S_{z3} r\mathrm{d}r \int_0^{2\pi}\mathrm{d}\phi\right)^2}. \end{aligned} \tag{8}$$

Here, $n_2 = 2.6 \times 10^{-20}\ m^2/w$ is the nonlinear refractive index.[13] In our calculations, we assume that the n_2 of air is negligible compared to that of silica. So the integral in the numerator is evaluated only over the dielectric region.[5]

We assume that the refractive index of the air is 1.0, so $n_1 = n_3 = 1.0$. Then we can use the following Sellmeier-type dispersion formula (at room temperature) to obtain the refractive indices of the dielectric material for fused silica (SiO_2):[6]

$$n^2 - 1 = \frac{0.6961663\lambda^2}{\lambda^2 - (0.0684043)^2} + \frac{0.4079426\lambda^2}{\lambda^2 - (0.1162414)^2} + \frac{0.8974794\lambda^2}{\lambda^2 - (9.896161)^2}. \quad (9)$$

Here, the unit of λ is μm.

3. Results and discussion

After the radius (b) of the dielectric region is designated as 200 nm, we calculate the wavelength-dependent MFD of the fundamental mode of ACNW for a different radius (a) of air core as shown in Fig.2. When the radius of the air core is given, the MFD increases with increasing wavelength. For a different radius (a) of the air core, the MFD is almost the same for shorter wavelengths (less than 0.7 μm), while the MFD scales quickly with the increase of the air-core radius for longer wavelengths (more than 0.8 μm). Therefore, we can conclude that ACNWs with smaller air-core radius (a) can achieve a tighter confinement of light.

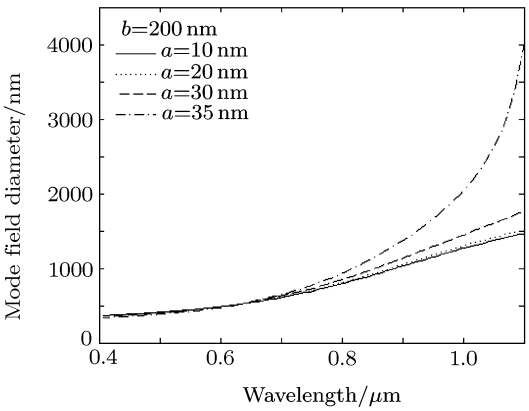


Fig.2. Wavelength-dependent MFD of fundamental mode of ACNW for a different core radius a.

We have also studied the wavelength-dependent MFD of fundamental mode of ACNW for a different radius (b) of the dielectric region, the radius (a) of the air core being assumed to be 10 nm. The results are shown in Fig.3. For a certain b, the MFD increases with increasing wavelength. This is due to the fact that the ACNW has a large portion of light left to be guided outside as evanescent waves when the wavelength is much larger than the radius (b) of the dielectric region.[6] For a different b, the MFD increases with b in the short wavelength region (e.g. from 0.4 μm to 0.6 μm), while the MFD decreases with increasing b in the long wavelength region (larger than 1 μm).

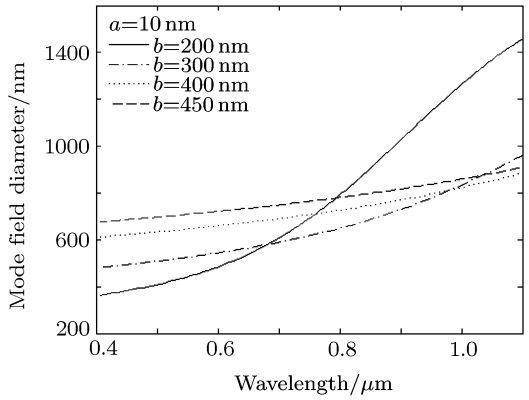


Fig.3. Wavelength-dependent MFD of fundamental mode of ACNW for a different radius b of the dielectric region.

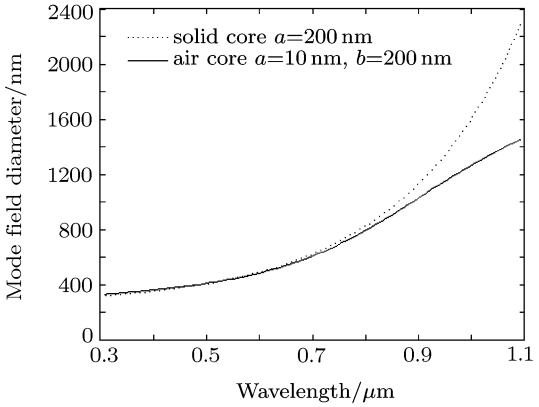


Fig.4. Wavelength-dependent MFD of fundamental mode of solid-core nanowire with air-cladding (dotted) and ACNW (solid) with the same radius of the dielectric region.

For comparison, wavelength-dependent MFDs of fundamental mode of ACNW and air-cladding solid-core silica nanowire with the same radius of the dielectric region are also simulated, as illustrated in Fig.4. The radius of dielectric region of both kinds of nanowire is assumed to be 200 nm, and the air-core radius (a) of ACNW is set to 10 nm. It is shown that both kinds of nanowire have almost the same MFD in the shorter wavelength region (from 0.3 μm to 0.65 μm) whereas the MFD of ACNW is obviously less than that of a solid-core nanowire in the longer wavelength region (from 0.7 μm to 1.1 μm). For example, at a wavelength of 1-μm, the MFD of ACNW is 1273 nm while the MFD of solid-core silica nanowire is 1624 nm. The existence of the small central air core

(e.g.10 nm) enhances the light confinement ability of the ACNWs.

Figure 5 shows the wavelength-dependent nonlinear coefficient of the fundamental mode of ACNW for a different air-core radius (a). Here the radius (b) of the dielectric region is assumed to be 200 nm. We can see from Fig.5 that the nonlinear coefficient of ACNW can be very large (e.g. an order of magnitude 10^4) compared with those of conventional fibers. The enhanced nonlinearity of ACNW may greatly advance the development of nonlinear optics. Numerical results also show that, at a particular core radius (a), the nonlinear coefficient decreases with the increase of the wavelength. The nonlinear coefficient increases with the decrease of the radius (a) of the air core in the short wavelength region (e.g. from 0.4 μm to 0.8 μm), while the nonlinear parameters of ACNWs with different air-core radius (a) are slightly different in the long wavelength region (e.g. larger than 0.8 μm). Therefore, in the visible light region we can enhance the nonlinearity of ACNW through decreasing the air-core radius.

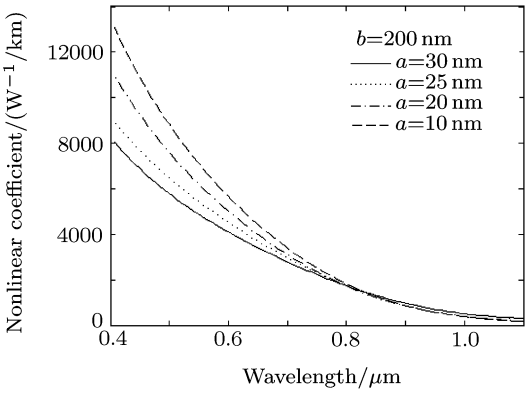


Fig.5. Wavelength-dependent nonlinear coefficient of fundamental mode of ACNW for a different core radius a.

The wavelength-dependent nonlinear coefficient of fundamental mode of ACNW for the radius (b) of the dielectric region is shown in Fig.6, where the air-core radius (a) of the ACNW is assumed to be 10 nm. From Fig.6, we can see that the nonlinear coefficient decreases with the increase of the wavelength at a particular b and the ACNW has weak optical light confinement ability for longer wavelengths. Meanwhile, the nonlinear coefficient of ACNW increases significantly with the decrease of the radius (b) of the dielectric region in the short wavelength region (shorter than 0.7 μm), while the nonlinear coefficient for small b (e.g. b=200 nm) decreases faster than that for large b in the long wavelength region (e.g. larger than 0.9 μm). The reasons can be explained by Fig.3.

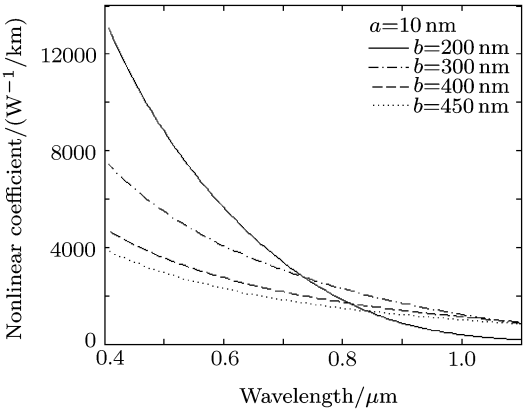


Fig.6. Wavelength-dependent nonlinear coefficient of fundamental mode of ACNW for different radius b of the dielectric region.

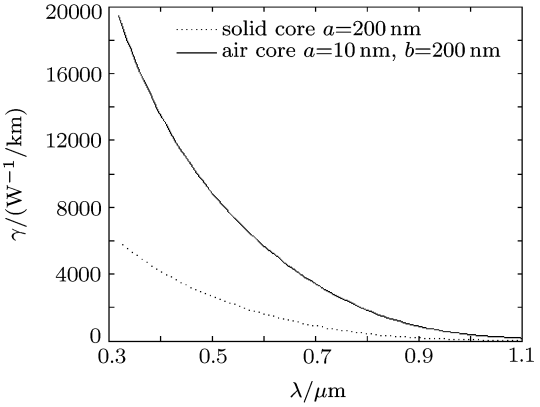


Fig.7. Wavelength-dependent nonlinear coefficient of fundamental mode of solid-core (dotted) and ACNW for the same radius of the dielectric region.

For comparison, the wavelength-dependent nonlinear coefficients of fundamental mode of ACNW and air-cladding solid-core silica nanowire are simulated, as shown in Fig.7. The radius of dielectric region of both kinds of nanowires is designated as 200 nm, and the air-core radius (a) of ACNW is set to 10 nm. One can see from Fig.7 that the nonlinear coefficient of ACNW is much larger than that of solid-core nanowire. It comes from the fact that the light intensity in the central hollow region of ACNW with a = 10 nm has been enhanced. The enhanced intensity results from the discontinuity of the electric field at the interface between the hollow region and the dielectric region.[14,15] Meanwhile, the nonlinear coefficient of the air-cladding solid-core silica wire decreases to zero quickly with the increase of the wavelength. Because of the larger wavelength, the air-cladding solid-core nanowire has a large portion of light left to be outside as evanescent waves.[6]

Figure 8 shows the dielectric region radius (b) dependent MFDs of fundamental mode of ACNWs at λ=800 nm. Here the air-core radius is assumed to be 10 nm. The minimum MFD is 646.5 nm for a radius of the dielectric region of 280 nm. After the minimum value, the MFD increases linearly with the radius of the dielectric region. When the radius of the dielectric region is smaller than the optimal value corresponding to the minimum MFD, further decrease in the dielectric region radius results in a rapid increase of MFD.

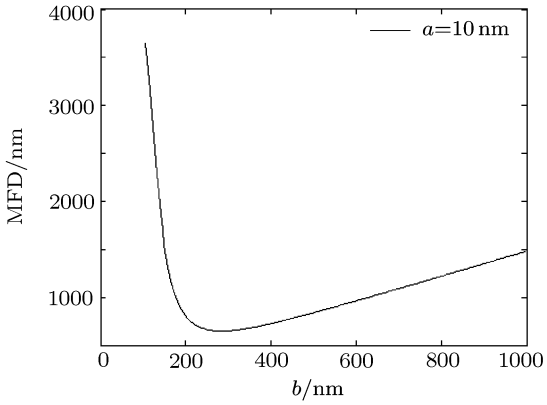


Fig.8. Dielectric region radius-dependent MFD of fundamental mode of ACNW with wavelength λ=800 nm.

The dielectric region radius (b) dependent nonlinear coefficients of fundamental mode of ACNWs are simulated for λ=800 nm. The numerical results are demonstrated in Fig.9, where the air-core radius is assumed to be 10 nm. The peak value for the nonlinear coefficient of 2406 W^{-1}/km occurs at a dielectric region radius of 263 nm. It is noticed that the smallest MFD does not necessarily correspond to the maximum nonlinearity. This is because the mode does not maintain a consistent shape as the fiber structure (e.g. the dielectric region radius) changes.[5] At λ=800 nm, the nonlinear coefficient of 2-μm core fiber is 114 W^{-1}/km.[5] For a=10 nm, the ACNW with the optimal dielectric region radius could yield approximately 21× larger effective nonlinearity at this wavelength. So the ACNWs are a powerful tool for nonlinear optics research.

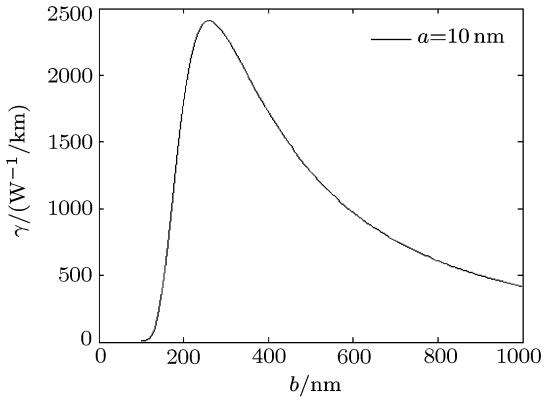


Fig.9. Dielectric region radius-dependent nonlinear coefficient of fundamental mode of ACNW for wavelength λ=800 nm.

4. Conclusions

Using the 3-layer-structured cylindrical waveguide model, we have investigated numerically the mode field diameter and nonlinear properties of ACNWs. We assume that the wires are ideally uniform in terms of diameter uniformity and sidewall smoothness. In comparison with conventional large-diameter fibers, ACNWs offer unique and excellent optical properties, such as extremely high nonlinearity. Meanwhile, by properly designing the geometrical parameters of ACNWs, we can maximize the nonlinearity and minimize the mode field diameter at a certain wavelength. ACNWs will be powerful potential tools for novel nonlinear phenomena and high-performance miniaturized photonic devices

References

[1] Zhou X J, Du D and Gong J J 2005 *Acta Phys. Sin.* **54** 2106 (in Chinese)
[2] Guo W G, Yang X F, Luo S J, Li Y N, Tu C H, Lü F Y, Wang H J, Li N B and Lü C 2007 *Acta Phys. Sin.* **56** 308 (in Chinese)
[3] Zhao C J, Tang Z X, Ye Y X, Fan D Y, Qian L J, Wen S C and Chen G H 2007 *Opt. Express* **15** 6629
[4] Lou J Y, Tong L M and Ye Z Z 2006 *Opt. Express* **14** 6993
[5] Foster M A, Moll K D and Gaeta A L 2004 *Opt. Express* **12** 2880
[6] Tong L M, Lou J Y and Mazur E 2004 *Opt. Express* **12** 1025
[7] Foster M A, Turner A C, Lipson M and Gaeta A L 2008 *Opt. Express* **16** 1300
[8] Gu X K and Cao B Y 2007 *Chin. Phys.* **16** 3777
[9] Tong L M, Gattass R R, Ashcom J B, He S L, Lou J Y, Shen M Y, Maxwell I and Mazur E 2003 *Nature* **426** 816
[10] Leon-Saval S G, Birks T A, Wadsworth W J and St J Russell P 2004 *Opt. Express* **12** 2864
[11] Huang L M, Wang H T, Hayashi C Y, Tian B Z, Zhao D Y and Yan Y S 2003 *J. Mater. Chem.* **13** 666
[12] Penman D 2003 *New Scientist* **12**
[13] Agrawal G P 2001 *Nonlinear Fiber Optics* (New York: Academic) p451
[14] Almeida V R, Xu Q, Barrios C A and Lipson M 2004 *Opt. Lett.* **29** 1209
[15] Wiederhecker G S, Cordeiro C M B, Couny F, Benabid F, Maier S A, Knight J C, Cruz C H B and Fragnito H L 2007 *Nature Photonics* **1** 115